

ETsformer: Exponential Smoothing Transformers for Time-series Forecasting

Gerald Woo^{1,2} Chenghao Liu¹ Doyen Sahoo¹ Akshat Kumar² Steven Hoi¹

Abstract

Transformers have been actively studied for time-series forecasting in recent years. While often showing promising results in various scenarios, traditional Transformers are not designed to fully exploit the characteristics of time-series data and thus suffer some fundamental limitations, e.g., they generally lack of decomposition capability and interpretability, and are neither effective nor efficient for long-term forecasting. In this paper, we propose ETSFormer, a novel time-series Transformer architecture, which exploits the principle of exponential smoothing in improving Transformers for time-series forecasting. In particular, inspired by the classical exponential smoothing methods in time-series forecasting, we propose the novel exponential smoothing attention (ESA) and frequency attention (FA) to replace the self-attention mechanism in vanilla Transformers, thus improving both accuracy and efficiency. Based on these, we redesign the Transformer architecture with modular decomposition blocks such that it can learn to decompose the time-series data into interpretable time-series components such as level, growth and seasonality. Extensive experiments on various time-series benchmarks validate the efficacy and advantages of the proposed method. The code and models of our implementations will be released.

1. Introduction

Transformer models have achieved great success in the fields of NLP (Vaswani et al., 2017; Devlin et al., 2019) and CV (Carion et al., 2020; Dosovitskiy et al., 2021) in recent times. The success is widely attributed to its self-attention mechanism which is able to explicitly model both short and long range dependencies adaptively via the pairwise query-key interaction. Owing to their powerful capability to model

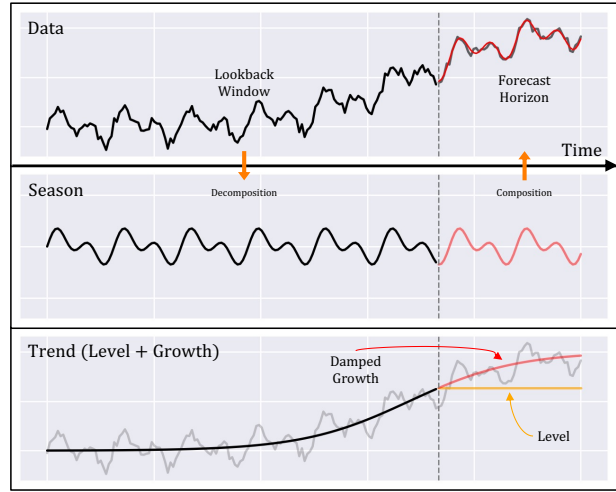


Figure 1. Illustration demonstrating how ETSformer generates forecasts via a decomposition (of intermediate representations) into seasonal and trend components. The seasonal component extracts salient periodic patterns and extrapolates them. The trend component which is a combination of the level and growth terms, first estimates the current level of the time-series, and subsequently adds a damped growth term to generate trend forecasts.

sequential data, Transformer-based architectures (Li et al., 2019; Wu et al., 2020; Zhou et al., 2021; Wu et al., 2021; Zerveas et al., 2021) have been actively explored for the time-series forecasting, especially for the more challenging Long Sequence Time-series Forecasting (LSTF) task. While showing promising results, it is still quite challenging to extract salient temporal patterns and thus make accurate long-term forecasts for large-scale data. This is because time-series data is usually noisy and non-stationary. Without incorporating appropriate knowledge about time-series structures (Assimakopoulos & Nikolopoulos, 2000; Theodosiou, 2011; Hyndman et al., 2008), it is prone to learning the spurious dependencies and lacks interpretability.

Moreover, the use of content-based, dot-product attention in Transformers is not effective in detecting essential temporal dependencies for two reasons. (1) Firstly, time-series data is usually assumed to be generated by a conditional distribution over past observations, with the dependence between observations weakening over time (Mohri & Rostamizadeh, 2010; Kuznetsov & Mohri, 2015). Therefore, neighboring data points have similar values, and recent tokens should

¹Salesforce Research Asia ²School of Computing and Information Systems, Singapore Management University. Correspondence to: Gerald Woo <gwoo@salesforce.com>.

be given a higher weight¹ when measuring their similarity (Hyndman et al., 2008; Hyndman & Khandakar, 2008). This indicates that attention measured by a relative time lag is more effective than that measured by the similarity of the content when modeling time-series. (2) Secondly, many real world time-series display strong seasonality – patterns in time-series which repeat with a fixed period. Automatically extracting seasonal patterns has been proved to be critical for the success of forecasting (Cleveland & Tiao, 1976; Cleveland et al., 1990). However, the vanilla attention mechanism is unlikely able to learn these required periodic dependencies without any in-built prior structure.

To address these limitations, we propose ETSformer, an effective and efficient Transformer architecture for time-series forecasting, inspired by exponential smoothing methods (Hyndman et al., 2008) and illustrated in Figure 1. First of all, ETSformer incorporates inductive biases of time-series structures by performing a layer-wise level, growth, and seasonal decomposition. By leveraging the high capacities of deep architectures and an effective residual learning scheme, ETSformer is able to extract a series of latent growth and seasonal patterns and model their complex dependencies. Secondly, ETSformer introduces a novel Exponential Smoothing Attention (ESA) and Frequency Attention (FA) to replace vanilla attention. In particular, ESA constructs attention scores based on the relative time lag to the query, and achieves $\mathcal{O}(L \log L)$ complexity for the length- L lookback window and demonstrates powerful capability in modeling the growth component. FA leverages the Fourier transformation to extract the dominating seasonal patterns by selecting the Fourier bases with the K largest amplitudes in frequency domain, and also achieves $\mathcal{O}(L \log L)$ complexity. Finally, the predicted forecast is a composition of level, trend, and seasonal components, which makes it human interpretable. We conduct extensive empirical analysis and show that ETSformer achieves state-of-the-art performance by outperforming competing approaches over 6 real world datasets on both the multivariate and univariate settings, and also visualize the time-series components to verify its interpretability.

2. Related Work

Transformer based deep forecasting. Inspired by the success of Transformers in CV and NLP, Transformer-based time-series forecasting models have been actively studied recently. LogTrans (Li et al., 2019) introduces local context to Transformer models via causal convolutions in the query-key projection layer, and propose the LogSparse attention to reduce complexity to $\mathcal{O}(L \log L)$. Informer (Zhou et al.,

¹An assumption further supported by the success of classical exponential smoothing methods and ARIMA model selection methods tending to select small lags.

2021) extends the Transformer by proposing the ProbSparse attention and distillation operation to achieve $\mathcal{O}(L \log L)$ complexity. AST (Wu et al., 2020) leverages a sparse normalization transform, α -entmax, to implement a sparse attention layer. It further incorporates an adversarial loss to mitigate the adverse effect of error accumulation in inference. Similar to our work that incorporates prior knowledge of time-series structure, Autoformer (Wu et al., 2021) introduces the Auto-Correlation attention mechanism which focuses on sub-series based similarity and is able to extract periodic patterns. Yet, their implementation of series decomposition which performs de-trending via a simple moving average over the input signal without any learnable parameters is arguably a simplified assumption, insufficient to appropriately model complex trend patterns. ETSformer on the other hand, decomposes the series by de-seasonalization as seasonal patterns are more identifiable and easier to detect (De Livera et al., 2011). Furthermore, the Auto-Correlation mechanism fails to attend to information from the local context (i.e. forecast at $t + 1$ is not dependent on $t, t - 1$, etc.) and does not separate the trend component into level and growth components, which are both crucial for modeling trend patterns. Lastly, similar to previous work, their approach is highly reliant on manually designed dynamic time-dependent covariates (e.g. month-of-year, day-of-week), while ETSformer is able to automatically learn and extract seasonal patterns from the time-series signal directly.

Attention Mechanism. The self-attention mechanism in Transformer models has recently received much attention, its necessity has been greatly investigated in attempts to introduce more flexibility and reduce computational cost. Synthesizer (Tay et al., 2021) empirically studies the importance of dot-product interactions, and show that a randomly initialized, learnable attention mechanisms with or without token-token dependencies can achieve competitive performance with vanilla self-attention on various NLP tasks. (You et al., 2020) utilizes an unparameterized Gaussian distribution to replace the original attention scores, concluding that the attention distribution should focus on a certain local window and can achieve comparable performance. (Raganato et al., 2020) replaces attention with fixed, non-learnable positional patterns, obtaining competitive performance on NMT tasks. (Lee-Thorp et al., 2021) replaces self-attention with a non-learnable Fourier Transform and verifies it to be an effective mixing mechanism. While our proposed ESA shares the spirit of designing attention mechanisms that are not dependent on pair-wise query-key interactions, our work is inspired by exploiting the characteristics of time-series and is an early attempt to utilize prior knowledge of time-series for tackling the time-series forecasting tasks.

3. Preliminaries and Background

Problem Formulation Let $x_t \in \mathbb{R}^m$ denote an observation of a multivariate time-series at time step t . Given a lookback window $\mathbf{X}_{t-L:t} = [x_{t-L}, \dots, x_{t-1}]$, we consider the task of predicting future values over a horizon, $\mathbf{X}_{t:t+H} = [x_t, \dots, x_{t+H-1}]$. We denote $\hat{\mathbf{X}}_{t:t+H}$ as the point forecast of $\mathbf{X}_{t:t+H}$. Thus, the goal is to learn a forecasting function $\hat{\mathbf{X}}_{t:t+H} = f(\mathbf{X}_{t-L:t})$ by minimizing some loss function $\mathcal{L} : \mathbb{R}^{H \times m} \times \mathbb{R}^{H \times m} \rightarrow \mathbb{R}$.

Exponential Smoothing We instantiate exponential smoothing methods (Hyndman et al., 2008) in the univariate forecasting setting. They assume that time-series can be decomposed into seasonal and trend components, and trend can be further decomposed into level and growth components. Specifically, a commonly used model is the additive Holt-Winters’ method (Holt, 2004; Winters, 1960), which can be formulated as:

$$\begin{aligned} \text{Level} : e_t &= \alpha(x_t - s_{t-p}) + (1 - \alpha)(e_{t-1} + b_{t-1}) \\ \text{Growth} : b_t &= \beta(e_t - e_{t-1}) + (1 - \beta)b_{t-1} \\ \text{Seasonal} : s_t &= \gamma(x_t - e_t) + (1 - \gamma)s_{t-p} \\ \text{Forecasting} : \hat{x}_{t+h|t} &= e_t + h b_t + s_{t+h-p} \end{aligned} \quad (1)$$

where p is the period of seasonality, and $\hat{x}_{t+h|t}$ is the h -steps ahead forecast. The above equations state that the h -steps ahead forecast is composed of the last estimated level e_t , incrementing it by h times the last growth factor, b_t , and adding the last available seasonal factor s_{t+h-p} . Specifically, the level smoothing equation is formulated as a weighted average of the seasonally adjusted observation ($x_t - s_{t-p}$) and the non-seasonal forecast, obtained by summing the previous level and growth ($e_{t-1} + b_{t-1}$). The growth smoothing equation is implemented by a weighted average between the successive difference of the (de-seasonalized) level, ($e_t - e_{t-1}$), and the previous growth, b_{t-1} . Finally, the seasonal smoothing equation is a weighted average between the difference of observation and (de-seasonalized) level, ($x_t - e_t$), and the previous seasonal index s_{t-p} . The weighted average of these three equations are controlled by the smoothing parameters α, β and γ , respectively.

A widely used modification of the additive Holt-Winters’ method is to allow the damping of trends, which has been proved to produce robust multi-step forecasts (Svetunkov, 2016; McKenzie & Gardner Jr, 2010). The forecast with damping trend can be rewritten as:

$$\hat{x}_{t+h|t} = e_t + (\phi + \phi^2 + \dots + \phi^h)b_t + s_{t+h-p}, \quad (2)$$

where the growth is damped by a factor of ϕ . If $\phi = 1$, it degenerates to the vanilla forecast. For $0 < \phi < 1$, as $h \rightarrow \infty$ this growth component approaches an asymptote given by $\phi b_t / (1 - \phi)$.

4. ETSformer

In this section, we redesign the classical Transformer architecture into an exponential smoothing inspired encoder-decoder architecture specialized for tackling the time-series forecasting problem. Our architecture design methodology relies on three key principles: (1) the architecture leverages the stacking of multiple layers to progressively extract a series of level, growth, and seasonal representations from the intermediate latent residual; (2) following the spirit of exponential smoothing, we extract the salient seasonal patterns while modeling level and growth components by assigning higher weight to recent observations; (3) the final forecast is a composition of level, growth, and seasonal components making it human interpretable. We now expound how our ETSformer architecture encompasses these principles.

4.1. Overall Architecture

Figure 2 illustrates the overall encoder-decoder architecture of ETSformer. At each layer, the encoder is designed to iteratively extract growth and seasonal latent components from the lookback window. The level is then extracted in a similar fashion to the level smoothing equation in 1. These extracted components are then fed to the decoder to further generate the final H -step ahead forecast via a composition of level, growth, and seasonal forecasts, which is defined:

$$\hat{\mathbf{X}}_{t:t+H} = \mathbf{E}_{t:t+H} + \text{Linear} \left(\sum_{n=1}^N (\mathbf{B}_{t:t+H}^{(n)} + \mathbf{S}_{t:t+H}^{(n)}) \right), \quad (3)$$

where $\mathbf{E}_{t:t+H} \in \mathbb{R}^{H \times m}$, and $\mathbf{B}_{t:t+H}^{(n)}, \mathbf{S}_{t:t+H}^{(n)} \in \mathbb{R}^{H \times d}$ represent the level forecasts, and the growth and seasonal latent representations of each time step in the forecast horizon, respectively. The superscript represents the stack index, for a total of N encoder stacks. Note that $\text{Linear}(\cdot) : \mathbb{R}^d \rightarrow \mathbb{R}^m$ operates element-wise along each time step, projecting the extracted growth and seasonal representations from latent to observation space.

4.1.1. INPUT EMBEDDING

Raw signals from the lookback window are mapped to latent space via the input embedding module, defined by $\mathbf{Z}_{t-L:t}^{(0)} = \mathbf{E}_{t-L:t}^{(0)} = \text{Conv}(\mathbf{X}_{t-L:t})$, where Conv is a temporal convolutional filter with kernel size 3, input channel m and output channel d . In contrast to prior work (Li et al., 2019; Wu et al., 2020, 2021; Zhou et al., 2021), the inputs of ETSformer do not rely on any other manually designed dynamic time-dependent covariates (e.g. month-of-year, day-of-week) for both the lookback window and forecast horizon. This is because the proposed Frequency Attention module (details in Section 4.2.2) is able to automatically uncover these seasonal patterns, which renders it more applicable for challenging scenarios without these discriminative covariates and reduces the need for feature engineering.

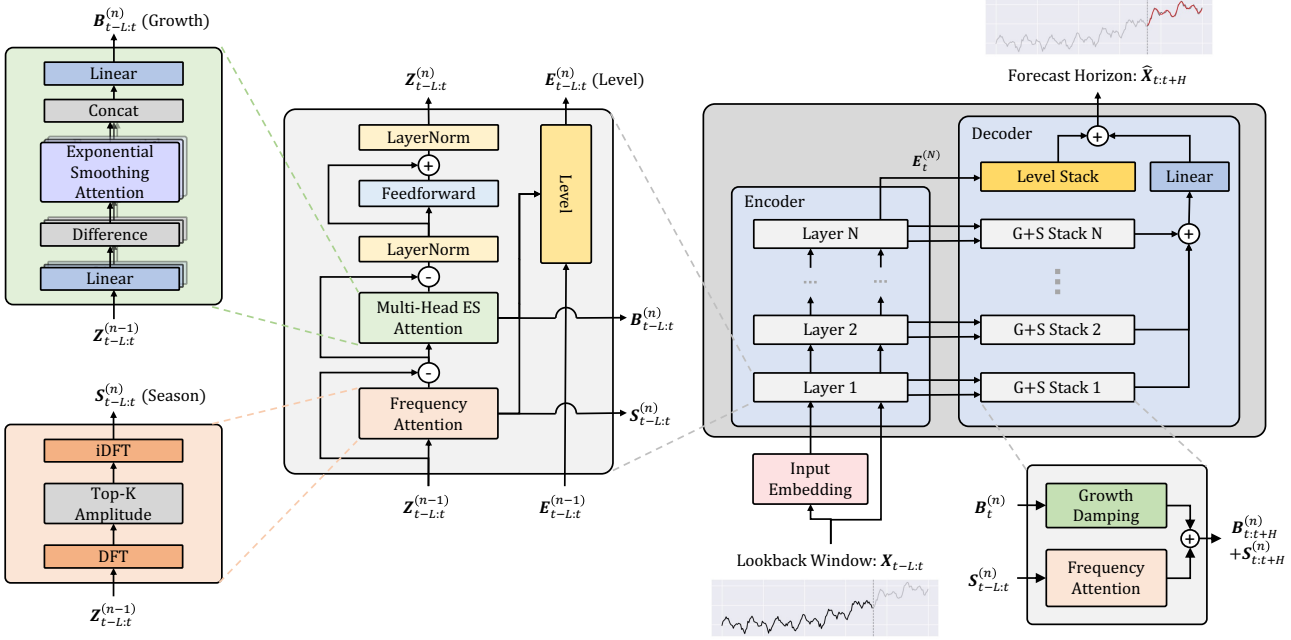


Figure 2. ETSformer model architecture.

4.1.2. ENCODER

The encoder focuses on extracting a series of latent growth and seasonality representations in a cascaded manner from the lookback window. To achieve this goal, traditional methods rely on the assumption of additive or multiplicative seasonality which has limited capability to express complex patterns beyond these assumptions. Inspired by (Oreshkin et al., 2019; He et al., 2016), we leverage residual learning to build an expressive, deep architecture to characterize the complex intrinsic patterns. Each layer can be interpreted as sequentially analyzing the input signals. The extracted growth and seasonal signals are then removed from the residual and undergo a nonlinear transformation before moving to the next layer. Each encoder layer takes as input the residual from the previous encoder layer $Z_{t-L:t}^{(n-1)}$ and emits $Z_{t-L:t}^{(n)}, B_{t-L:t}^{(n)}, S_{t-L:t}^{(n)}$, the residual, latent growth, and seasonal representations for the lookback window via the Multi-Head Exponential Smoothing Attention (MH-ESA) and Frequency Attention (FA) modules (detailed description in Section 4.2). The following equations formalizes the overall pipeline in each encoder layer, and for ease of exposition, we use the notation $:=$ for a variable update.

$$\begin{aligned}
 \text{Seasonal: } S_{t-L:t}^{(n)} &= \text{FA}_{t-L:t}(Z_{t-L:t}^{(n-1)}) \\
 Z_{t-L:t}^{(n-1)} &:= Z_{t-L:t}^{(n-1)} - S_{t-L:t}^{(n)} \\
 \text{Growth: } B_{t-L:t}^{(n)} &= \text{MH-ESA}(Z_{t-L:t}^{(n-1)}) \\
 Z_{t-L:t}^{(n-1)} &:= \text{LN}(Z_{t-L:t}^{(n-1)} - B_{t-L:t}^{(n)}) \\
 Z_{t-L:t}^{(n)} &= \text{LN}(Z_{t-L:t}^{(n-1)} + \text{FF}(Z_{t-L:t}^{(n-1)}))
 \end{aligned}$$

LN is layer normalization (Ba et al., 2016), $\text{FF}(x) = \text{Linear}(\sigma(\text{Linear}(x)))$ is a position-wise feedforward network (Vaswani et al., 2017) and $\sigma(\cdot)$ is the sigmoid function.

Level Module Given the latent growth and seasonal representations from each layer, we extract the level at each time step t in the lookback window in a similar way as the level smoothing equation in Equation (1). Formally, the adjusted level is a weighted average of the current (de-seasonalized) level and the level-growth forecast from the previous time step $t-1$. It can be formulated as:

$$\begin{aligned}
 E_t^{(n)} &= \alpha * (E_t^{(n-1)} - \text{Linear}(S_t^{(n)})) \\
 &+ (1 - \alpha) * (E_{t-1}^{(n)} + \text{Linear}(B_{t-1}^{(n)})),
 \end{aligned}$$

where $\alpha \in \mathbb{R}^m$ is a learnable smoothing parameter, $*$ is an element-wise multiplication term, and $\text{Linear}(\cdot) : \mathbb{R}^d \rightarrow \mathbb{R}^m$ maps representations to observation space. Finally, the extracted level in the last layer $E_{t-L:t}^{(N)}$ can be regarded as the corresponding level for the lookback window. We show in Appendix A.2 that this recurrent exponential smoothing equation can also be efficiently evaluated using the efficient \mathcal{A}_{ES} algorithm (Algorithm 1) with an auxiliary term.

4.1.3. DECODER

The decoder is tasked with generating the H -step ahead forecasts. As shown in Equation (3), the final forecast is a composition of level forecasts $E_{t:t+H}$, growth representations $B_{t:t+H}^{(n)}$ and seasonal representations $S_{t:t+H}^{(n)}$ in the forecast horizon. It comprises N Growth + Seasonal (G+S) Stacks,

and a Level Stack. The G+S Stack consists of the Growth Damping (GD) and FA blocks, which leverage $\mathbf{B}_t^{(n)}$, $\mathbf{S}_{t-L:t}^{(n)}$ to predict $\mathbf{B}_{t:t+H}^{(n)}$, $\mathbf{S}_{t:t+H}^{(n)}$, respectively.

$$\begin{aligned} \text{Growth: } \mathbf{B}_{t:t+H}^{(n)} &= \text{TD}(\mathbf{B}_t^{(n)}) \\ \text{Seasonal: } \mathbf{S}_{t:t+H}^{(n)} &= \text{FA}_{t:t+H}(\mathbf{S}_{t-L:t}^{(n)}) \end{aligned}$$

To obtain the level in the forecast horizon, the Level Stack repeats the level in the last time step t along the forecast horizon. It can be defined as $\mathbf{E}_{t:t+H} = \text{Repeat}_H(\mathbf{E}_t^{(N)}) = [\mathbf{E}_t^{(N)}, \dots, \mathbf{E}_t^{(N)}]$, with $\text{Repeat}_H(\cdot) : \mathbb{R}^{1 \times m} \rightarrow \mathbb{R}^{H \times m}$.

Growth Damping To obtain the growth representation in the forecast horizon, we follow the idea of trend damping in Equation (2) to make robust multi-step forecast. Thus, the trend representations can be formulated as:

$$\begin{aligned} \text{TD}(\mathbf{B}_t^{(n)})_j &= \sum_{i=1}^j \gamma^i \mathbf{B}_t^{(n)}, \\ \text{TD}(\mathbf{B}_{t-L:t}^{(n)}) &= [\text{TD}(\mathbf{B}_t^{(n)})_t, \dots, \text{TD}(\mathbf{B}_t^{(n)})_{t+H-1}], \end{aligned}$$

where $0 < \gamma < 1$ is the damping parameter which is learnable, and in practice, we apply a multi-head version of trend damping by making use of n_h damping parameters. Similar to the implementation for level forecast in the Level Stack, we only use the last trend representation in the lookback window $\mathbf{B}_t^{(n)}$ to forecast the trend representation in the forecast horizon.

4.2. Exponential Smoothing Attention and Frequency Attention Mechanism

Considering the ineffectiveness of existing attention mechanisms in handling time-series data, we develop the Exponential Smoothing Attention (ESA) and Frequency Attention (FA) mechanisms to extract latent growth and seasonal representations. ESA is a non-adaptive, learnable attention scheme with an inductive bias to attend more strongly to recent observations by following an exponential decay, while FA is a non-learnable attention scheme, that leverages Fourier transformation to select dominating seasonal patterns. A comparison between existing work and our proposed ESA and FA is illustrated in Figure 3.

4.2.1. EXPONENTIAL SMOOTHING ATTENTION

Vanilla self-attention can be regarded as a weighted combination of an input sequence, where the weights are normalized alignment scores measuring the similarity between input contents (Tsai et al., 2019). Inspired by the exponential smoothing in Equation (1), we aim to assign a higher weight to recent observations. It can be regarded as a novel form of attention whose weights are computed by the relative time lag, rather than input content. Thus, the ESA

Algorithm 1 PyTorch-style pseudocode of efficient \mathcal{A}_{ES}

conv1d_fft: efficient convolution operation implemented with fast Fourier transform (Appendix A, Algorithm 3), outer: outer product

```
# V: value matrix, shape: L x d
# v0: initial state, shape: d
# alpha: smoothing parameter, shape: 1

# obtain exponentially decaying weights
# and compute weighted combination
powers = arange(L) # L
weight = alpha * (1 - alpha) ** flip(powers) # L
output = conv1d_fft(V, weight, dim=0) # L x d

# compute contribution from initial state
init_weight = (1 - alpha) ** (powers + 1) # L
init_output = outer(init_weight, v0) # L x d
return init_output + output
```

mechanism can be defined as $\mathcal{A}_{\text{ES}} : \mathbb{R}^{L \times d} \rightarrow \mathbb{R}^{L \times d}$, where $\mathcal{A}_{\text{ES}}(\mathbf{V})_t \in \mathbb{R}^d$ denotes the t -th row of the output matrix, representing the token corresponding to the t -th time step. Its exponential smoothing formula can be further written as:

$$\begin{aligned} \mathcal{A}_{\text{ES}}(\mathbf{V})_t &= \alpha \mathbf{V}_t + (1 - \alpha) \mathcal{A}_{\text{ES}}(\mathbf{V})_{t-1}, \\ &= \sum_{j=0}^{t-1} \alpha (1 - \alpha)^j \mathbf{V}_{t-j} + (1 - \alpha)^t \mathbf{v}_0, \end{aligned}$$

where $0 < \alpha < 1$ and \mathbf{v}_0 are learnable parameters known as the smoothing parameter and initial state respectively.

Efficient \mathcal{A}_{ES} algorithm The straightforward implementation of the ESA mechanism by constructing the attention matrix, \mathbf{A}_{ES} and performing a matrix multiplication with the input sequence (detailed algorithm in Appendix A.1) results in an $\mathcal{O}(L^2)$ computational complexity.

$$\begin{aligned} \mathcal{A}_{\text{ES}}(\mathbf{V}) &= \begin{bmatrix} \mathcal{A}_{\text{ES}}(\mathbf{V})_1 \\ \vdots \\ \mathcal{A}_{\text{ES}}(\mathbf{V})_L \end{bmatrix} = \mathbf{A}_{\text{ES}} \cdot \begin{bmatrix} \mathbf{v}_0^T \\ \mathbf{V} \end{bmatrix}, \\ \mathbf{A}_{\text{ES}} &= \begin{bmatrix} (1 - \alpha)^1 & \alpha & 0 & 0 & \dots & 0 \\ (1 - \alpha)^2 & \alpha(1 - \alpha) & \alpha & 0 & \dots & 0 \\ (1 - \alpha)^3 & \alpha(1 - \alpha)^2 & \alpha(1 - \alpha) & \alpha & \dots & 0 \\ \vdots & \vdots & \vdots & \vdots & \ddots & \vdots \\ (1 - \alpha)^L & \alpha(1 - \alpha)^{L-1} & \dots & \alpha(1 - \alpha)^j & \dots & \alpha \end{bmatrix}. \end{aligned}$$

Yet, we are able to achieve an efficient algorithm by exploiting the unique structure of the exponential smoothing attention matrix, \mathbf{A}_{ES} . Each row of the attention matrix can be regarded as iteratively right shifting with padding (ignoring the first column). Thus, a matrix-vector multiplication can be computed with a cross-correlation operation, which in turn has an efficient fast Fourier transform implementation (Mathieu et al., 2014). The full algorithm is described in Algorithm 1, achieving an $\mathcal{O}(L \log L)$ complexity.

Multi-Head Exponential Smoothing Attention (MH-ESA) We use \mathcal{A}_{ES} as a basic building block, and develop the

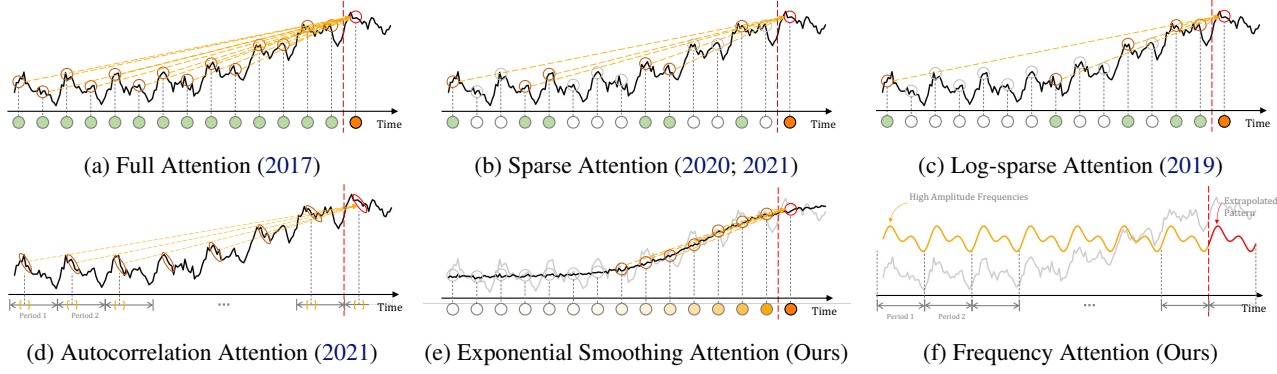


Figure 3. Comparison between different attention mechanisms. (a) Full, (b) Sparse, and (c) Log-sparse Attentions are adaptive mechanisms, where the green circles represent the attention weights adaptively calculated by a point-wise dot-product query, and depends on various factors including the time-series value, additional covariates (e.g. positional encodings, time features, etc.). (d) Autocorrelation attention considers sliding dot-product queries to construct attention weights for each rolled input series. We introduce (e) Exponential Smoothing Attention (ESA) and (f) Frequency Attention (FA). ESA directly computes attention weights based on the relative time lag, without considering the input content, while FA attends to patterns which dominate with large magnitudes in the frequency domain.

Multi-Head Exponential Smoothing Attention to extract latent growth representations. Formally, we obtain the growth representations by taking the successive difference of the residuals.

$$\begin{aligned}\tilde{\mathbf{Z}}_{t-L:t}^{(n)} &= \text{Linear}(\mathbf{Z}_{t-L:t}^{(n-1)}), \\ \mathbf{B}_{t-L:t}^{(n)} &= \text{MH-}\mathcal{A}_{\text{ES}}(\tilde{\mathbf{Z}}_{t-L:t}^{(n)} - [\tilde{\mathbf{Z}}_{t-L:t-1}^{(n)}, \mathbf{v}_0^{(n)}]), \\ \mathbf{B}_{t-L:t}^{(n)} &:= \text{Linear}(\mathbf{B}_{t-L:t}^{(n)}),\end{aligned}$$

where $\text{MH-}\mathcal{A}_{\text{ES}}(\cdot)$ is a multi-head version of \mathcal{A}_{ES} and $\mathbf{v}_0^{(n)}$ is the initial state from the ESA mechanism.

4.2.2. FREQUENCY ATTENTION

The goal of identifying and extracting seasonal patterns from the lookback window is twofold. Firstly, it can be used to perform de-seasonalization on the input signals such that downstream components are able to focus on modeling the level and growth information. Secondly, we are able to extrapolate the seasonal patterns to build representations for the forecast horizon. The main challenge is to automatically identify seasonal patterns. Fortunately, the use of power spectral density estimation for periodicity detection has been well studied (Vlachos et al., 2005). Inspired by these methods, we leverage the discrete Fourier transform (DFT, details in Appendix B) to develop the FA mechanism to extract dominant seasonal patterns.

Specifically, FA first decomposes input signals into their Fourier bases via a DFT along the temporal dimension, $\mathcal{F}(\mathbf{Z}_{t-L:t}^{(n-1)}) \in \mathbb{C}^{F \times d}$ where $F = \lfloor L/2 \rfloor + 1$, and selects bases with the K largest amplitudes. An inverse DFT is then applied to obtain the seasonality pattern in time domain.

Formally, this is given by the following equations:

$$\begin{aligned}\Phi_{k,i} &= \phi\left(\mathcal{F}(\mathbf{Z}_{t-L:t}^{(n-1)})_{k,i}\right), \quad \mathbf{A}_{k,i} = \left|\mathcal{F}(\mathbf{Z}_{t-L:t}^{(n-1)})_{k,i}\right|, \\ \kappa_i^{(1)}, \dots, \kappa_i^{(K)} &= \arg \text{Top-K} \left\{ \mathbf{A}_{k,i} \right\}, \\ \mathbf{S}_{j,i}^{(n)} &= \sum_{k=1}^K \mathbf{A}_{\kappa_i^{(k)},i} \left[\cos(2\pi f_{\kappa_i^{(k)}} j + \Phi_{\kappa_i^{(k)},i}) + \cos(2\pi \bar{f}_{\kappa_i^{(k)}} j + \bar{\Phi}_{\kappa_i^{(k)},i}) \right],\end{aligned}\quad (4)$$

where $\Phi_{k,i}, \mathbf{A}_{k,i}$ are the phase/amplitude of the k -th frequency for the i -th dimension, $\arg \text{Top-K}$ returns the arguments of the top K amplitudes, K is a hyperparameter, f_k is the Fourier frequency of the corresponding index, and $\bar{f}_k, \bar{\Phi}_{k,i}$ are the Fourier frequency/amplitude of the corresponding conjugates.

Finally, the latent seasonal representation of the i -th dimension for the lookback window is formulated as $\mathbf{S}_{t-L:t,i}^{(n)} = [\mathbf{S}_{t-L,i}^{(n)}, \dots, \mathbf{S}_{t-1,i}^{(n)}]$. For the forecast horizon, the FA module extrapolates beyond the lookback window via, $\mathbf{S}_{t:t+H,i}^{(n)} = [\mathbf{S}_{t,i}^{(n)}, \dots, \mathbf{S}_{t+H-1,i}^{(n)}]$. Since K is a hyperparameter typically chosen for small values, the complexity for the FA mechanism is similarly $\mathcal{O}(L \log L)$.

5. Experiments

This section presents extensive empirical evaluations on the LSTF task over 6 real world datasets, ETT, ECL, Exchange, Traffic, Weather, and ILI, coming from a variety of application areas (details in Appendix D) for both multivariate and univariate settings. This is followed by an ablation study of the various contributing components, an analysis on the computational efficiency, and interpretability experiments of our proposed model. For the main benchmark, datasets

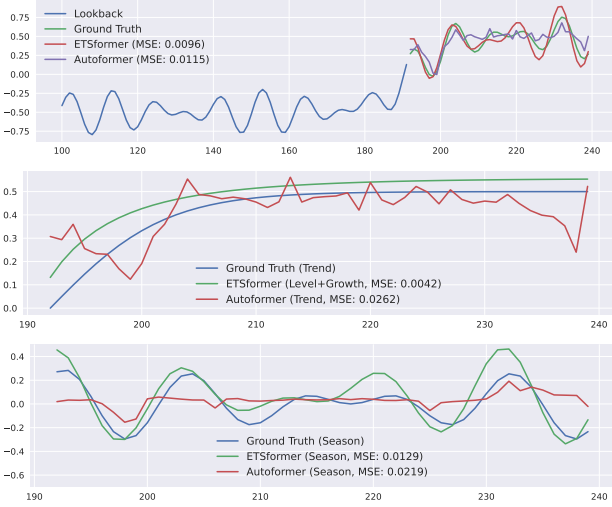


Figure 4. Visualization of decomposed forecasts from ETSformer and Autoformer on a synthetic dataset. The data sample on which Autoformer obtained lowest MSE was selected for visualization.

are split into train, validation, and test sets chronologically, following a 60/20/20 split for the ETT datasets and 70/10/20 split for other datasets. Inputs are zero-mean normalized and we use MSE and MAE as evaluation metrics. Further implementation details can be found in Appendix C.

5.1. Results

Tables 1 and 2 summarize the results of ETSformer against top performing baselines on a selection of datasets, for the multivariate and univariate settings respectively. A complete table of results for both settings can be found in Appendices F and G due to space constraints. For the multivariate benchmark, baselines include recently proposed time-series/efficient Transformers – Autoformer, Informer, LogTrans, and Reformer (Kitaev et al., 2020), and RNN variants – LSTnet (Lai et al., 2018), and LSTM (Hochreiter & Schmidhuber, 1997). Univariate baselines further include N-BEATS (Oreshkin et al., 2019), DeepAR (Salinas et al., 2020), ARIMA, and Prophet (Taylor & Letham, 2018).

Overall, ETSformer achieves state-of-the-art performance, achieving the best performance (across all datasets/settings, based on MSE) on 35 out of 40 settings for the multivariate case, and 17 out of 23 for the univariate case. Notably, on Exchange, a dataset with no obvious periodic patterns, ETSformer demonstrates an average (over forecast horizons) improvement of 39.8% over the best performing baseline, evidencing its strong trend forecasting capabilities.

5.2. Ablation Study

We study the contribution of each major component which the final forecast is composed of level, growth, and seasonality. Table 3 first presents the performance of the full model,

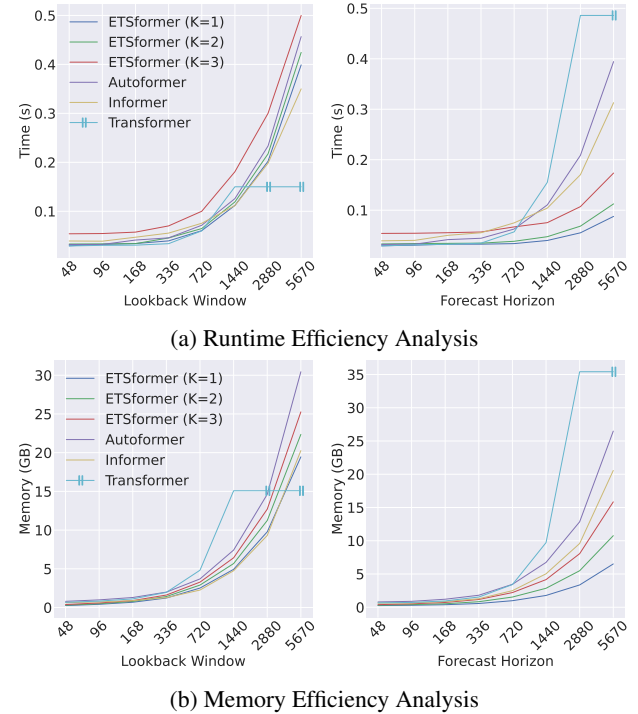


Figure 5. Computational Efficiency Analysis. Values reported are based on the training phase of ETTm2 multivariate setting. For runtime efficiency, values refer to the time for one iteration. The “||” marker indicates an out-of-memory error for those settings.

and subsequently, the performance of the resulting model by removing each component. We observe that the composition of level, growth, and season provides the most accurate forecasts across a variety of application areas, and removing any one component results in a deterioration. In particular, estimation of the level of the time-series is critical.

5.3. Interpretability

Figure 4 showcases how ETSformer generates forecasts based on a composition of interpretable time-series components. ETSformer is first trained on a synthetic dataset (details in Appendix E) which contains clear (nonlinear) trend and seasonality patterns. Given a lookback window (without noise), we visualize the forecast, as well as decomposed trend and seasonal forecasts. ETSformer successfully forecasts interpretable level, trend (level + growth), and seasonal components, as observed in the trend and seasonality components closely tracking the ground truth patterns. Despite obtaining a low MSE, the competing decomposition based approach, Autoformer, struggles to disambiguate between trend and seasonality.

5.4. Computational Efficiency

We compare the computational efficiency of ETSformer with competing Transformer-based approaches in Figure 5,

Table 1. Multivariate forecasting results over various forecast horizons, best results are highlighted in bold.

METHODS	ETSFOMER	AUTOFORMER	INFORMER	LOGTRANS	REFORMER	LSTNET	LSTM							
METRICS	MSE	MAE	MSE	MAE	MSE	MAE	MSE	MAE	MSE	MAE	MSE	MAE		
ETTM2	24	0.110 0.222	0.153	0.261	0.173	0.301	0.211	0.332	0.333	0.429	1.101	0.831	0.580	0.572
	48	0.142 0.250	0.178	0.280	0.303	0.409	0.427	0.487	0.558	0.571	2.619	1.393	0.747	0.630
	96	0.183 0.275	0.255	0.339	0.365	0.453	0.768	0.642	0.658	0.619	3.142	1.365	2.041	1.073
	288	0.291 0.339	0.342	0.378	1.047	0.804	1.090	0.806	2.441	1.190	2.856	1.329	0.969	0.742
	672	0.395 0.402	0.434	0.430	3.126	1.302	2.397	1.214	3.090	1.328	3.409	1.420	2.541	1.239
ECL	96	0.187 0.302	0.201	0.317	0.274	0.368	0.258	0.357	0.312	0.402	0.680	0.645	0.375	0.437
	192	0.196 0.311	0.222	0.334	0.296	0.386	0.266	0.368	0.348	0.433	0.725	0.676	0.442	0.473
	336	0.215 0.330	0.231	0.338	0.300	0.394	0.280	0.380	0.350	0.433	0.828	0.727	0.439	0.473
	720	0.236 0.348	0.254	0.361	0.373	0.439	0.283	0.376	0.340	0.420	0.957	0.811	0.980	0.814
EXCHANGE	96	0.083 0.202	0.197	0.323	0.847	0.752	0.968	0.812	1.065	0.829	1.551	1.058	1.453	1.049
	192	0.180 0.302	0.300	0.369	1.204	0.895	1.040	0.851	1.188	0.906	1.477	1.028	1.846	1.179
	336	0.354 0.433	0.509	0.524	1.672	1.036	1.659	1.081	1.357	0.976	1.507	1.031	2.136	1.231
	720	0.996 0.761	1.447	0.941	2.478	1.310	1.941	1.127	1.510	1.016	2.285	1.243	2.984	1.427
ILI	24	2.862 1.128	3.483	1.287	5.764	1.677	4.480	1.444	4.400	1.382	6.026	1.770	5.914	1.734
	36	2.683 1.029	3.103	1.148	4.755	1.467	4.799	1.467	4.783	1.448	5.340	1.668	6.631	1.845
	48	2.456 0.986	2.669	1.085	4.763	1.469	4.800	1.468	4.832	1.465	6.080	1.787	6.736	1.857
	60	2.630 1.057	2.770	1.125	5.264	1.564	5.278	1.560	4.882	1.483	5.548	1.720	6.870	1.879

Table 2. Univariate forecasting results over various forecast horizons, best results are highlighted in bold.

METHODS	ETSFOMER	AUTOFORMER	INFORMER	N-BEATS	DEEPAR	ARIMA	PROPHET							
METRICS	MSE	MAE	MSE	MAE	MSE	MAE	MSE	MAE						
ETTH2	24	0.089 0.234	0.106	0.255	0.093	0.24	0.198	0.345	0.098	0.263	3.554	0.445	0.199	0.381
	48	0.119 0.272	0.135	0.287	0.155	0.314	0.234	0.386	0.163	0.341	3.19	0.474	0.304	0.462
	168	0.199	0.360	0.186 0.341	0.232	0.389	0.331	0.453	0.255	0.414	2.8	0.595	2.145	1.068
	336	0.218 0.384	0.244	0.388	0.263	0.417	0.431	0.508	0.604	0.607	2.753	0.738	2.096	2.543
	720	0.216 0.378	0.299	0.440	0.277	0.431	0.437	0.517	0.429	0.58	2.878	1.044	3.355	4.664
EXCHANGE	96	0.126 0.268	0.241	0.387	0.591	0.615	0.156	0.299	0.417	0.515	0.112 0.245	0.828	0.762	
	192	0.206 0.341	0.273	0.403	1.183	0.912	0.669	0.665	0.813	0.735	0.304	0.404	0.909	0.974
	336	0.436 0.503	0.508	0.539	1.367	0.984	0.611	0.605	1.331	0.962	0.736	0.598	1.304	0.988
	720	1.320	0.887	0.991 0.768	1.872	1.072	1.111	0.860	1.894	1.181	1.871	0.935	3.238	1.566

Table 3. Ablation study on the various components of ETSformer. Experiments are performed on $H = 24$ forecast horizon setting.

DATASETS	ETTH2	ETTM2	ECL	TRAFFIC	
ETSFOMER	MSE	0.190	0.110	0.163	0.571
	MAE	0.296	0.222	0.287	0.373
W/O LEVEL	MSE	1.159	0.464	0.275	0.649
	MAE	0.878	0.518	0.373	0.393
W/O GROWTH	MSE	0.208	0.115	0.167	0.583
	MAE	0.300	0.226	0.288	0.383
W/O SEASON	MSE	0.204	0.131	0.696	1.334
	MAE	0.307	0.236	0.677	0.779

and show that ETSformer maintains competitive efficiency with competing quasilinear complexity Transformers while obtaining state-of-the-art performance. Furthermore, due to ETSformer’s unique decoder architecture which does not require output embeddings, but instead relies on its Trend Damping and Frequency Attention modules, ETSformer

maintains superior efficiency as forecast horizon increases.

6. Conclusion

Inspired by the classical exponential smoothing methods and emerging Transformer approaches for time-series forecasting, we proposed ETSformer, a novel Transformer-based architecture for time-series forecasting which learns level, growth, and seasonal latent representations and their complex dependencies. ETSformer leverages the novel Exponential Smoothing Attention and Frequency Attention mechanisms which are more effective at modeling time-series than vanilla self-attention mechanism, and at the same time achieves $\mathcal{O}(L \log L)$ complexity, where L is the length of lookback window. Finally, we perform extensive empirical evaluation in which ETSformer achieves state-of-the-art performance on six real world datasets by beating competing baselines in 35 out of 40 and 17 out of 23 settings for multivariate and univariate forecasting respectively.

References

Assimakopoulos, V. and Nikolopoulos, K. The theta model: a decomposition approach to forecasting. *International journal of forecasting*, 16(4):521–530, 2000.

Ba, J. L., Kiros, J. R., and Hinton, G. E. Layer normalization, 2016.

Carion, N., Massa, F., Synnaeve, G., Usunier, N., Kirillov, A., and Zagoruyko, S. End-to-end object detection with transformers. In *European Conference on Computer Vision*, pp. 213–229. Springer, 2020.

Cleveland, R. B., Cleveland, W. S., McRae, J. E., and Terpenning, I. Stl: A seasonal-trend decomposition. *J. Off. Stat.*, 6(1):3–73, 1990.

Cleveland, W. P. and Tiao, G. C. Decomposition of seasonal time series: a model for the census x-11 program. *Journal of the American statistical Association*, 71(355):581–587, 1976.

De Livera, A. M., Hyndman, R. J., and Snyder, R. D. Forecasting time series with complex seasonal patterns using exponential smoothing. *Journal of the American statistical association*, 106(496):1513–1527, 2011.

Devlin, J., Chang, M.-W., Lee, K., and Toutanova, K. Bert: Pre-training of deep bidirectional transformers for language understanding. *ArXiv*, abs/1810.04805, 2019.

Dosovitskiy, A., Beyer, L., Kolesnikov, A., Weissenborn, D., Zhai, X., Unterthiner, T., Dehghani, M., Minderer, M., Heigold, G., Gelly, S., Uszkoreit, J., and Houlsby, N. An image is worth 16x16 words: Transformers for image recognition at scale. In *International Conference on Learning Representations*, 2021. URL <https://openreview.net/forum?id=YicbFdNTTy>.

He, K., Zhang, X., Ren, S., and Sun, J. Deep residual learning for image recognition. In *Proceedings of the IEEE conference on computer vision and pattern recognition*, pp. 770–778, 2016.

Hochreiter, S. and Schmidhuber, J. Long short-term memory. *Neural computation*, 9(8):1735–1780, 1997.

Holt, C. C. Forecasting seasonals and trends by exponentially weighted moving averages. *International journal of forecasting*, 20(1):5–10, 2004.

Hyndman, R., Koehler, A. B., Ord, J. K., and Snyder, R. D. *Forecasting with exponential smoothing: the state space approach*. Springer Science & Business Media, 2008.

Hyndman, R. J. and Khandakar, Y. Automatic time series forecasting: the forecast package for r. *Journal of statistical software*, 27(1):1–22, 2008.

Kingma, D. P. and Ba, J. Adam: A method for stochastic optimization. In Bengio, Y. and LeCun, Y. (eds.), *3rd International Conference on Learning Representations, ICLR 2015, San Diego, CA, USA, May 7-9, 2015, Conference Track Proceedings*, 2015. URL <http://arxiv.org/abs/1412.6980>.

Kitaev, N., Kaiser, L., and Levskaya, A. Reformer: The efficient transformer. In *International Conference on Learning Representations*, 2020. URL <https://openreview.net/forum?id=rkgNKkHtvB>.

Kuznetsov, V. and Mohri, M. Learning theory and algorithms for forecasting non-stationary time series. In *NIPS*, pp. 541–549. Citeseer, 2015.

Lai, G., Chang, W.-C., Yang, Y., and Liu, H. Modeling long- and short-term temporal patterns with deep neural networks. In *The 41st International ACM SIGIR Conference on Research & Development in Information Retrieval*, pp. 95–104, 2018.

Lee-Thorp, J., Ainslie, J., Eckstein, I., and Ontanon, S. Fnet: Mixing tokens with fourier transforms. *arXiv preprint arXiv:2105.03824*, 2021.

Li, S., Jin, X., Xuan, Y., Zhou, X., Chen, W., Wang, Y.-X., and Yan, X. Enhancing the locality and breaking the memory bottleneck of transformer on time series forecasting. *ArXiv*, abs/1907.00235, 2019.

Mathieu, M., Henaff, M., and LeCun, Y. Fast training of convolutional networks through ffts. *CoRR*, abs/1312.5851, 2014.

McKenzie, E. and Gardner Jr, E. S. Damped trend exponential smoothing: a modelling viewpoint. *International Journal of Forecasting*, 26(4):661–665, 2010.

Mohri, M. and Rostamizadeh, A. Stability bounds for stationary φ -mixing and β -mixing processes. *Journal of Machine Learning Research*, 11(2), 2010.

Oreshkin, B. N., Carpov, D., Chapados, N., and Bengio, Y. N-beats: Neural basis expansion analysis for interpretable time series forecasting. In *International Conference on Learning Representations*, 2019.

Raganato, A., Scherrer, Y., and Tiedemann, J. Fixed encoder self-attention patterns in transformer-based machine translation. In Cohn, T., He, Y., and Liu, Y. (eds.), *Findings of the Association for Computational Linguistics: EMNLP 2020, Online Event, 16-20 November 2020*, volume EMNLP 2020 of *Findings of ACL*, pp. 556–568. Association for Computational Linguistics, 2020. doi: 10.18653/v1/2020.findings-emnlp.49. URL <https://doi.org/10.18653/v1/2020.findings-emnlp.49>.

Salinas, D., Flunkert, V., Gasthaus, J., and Januschowski, T. Deepar: Probabilistic forecasting with autoregressive recurrent networks. *International Journal of Forecasting*, 36(3):1181–1191, 2020. ISSN 0169-2070. doi: <https://doi.org/10.1016/j.ijforecast.2019.07.001>. URL <https://www.sciencedirect.com/science/article/pii/S0169207019301888>.

Srivastava, N., Hinton, G., Krizhevsky, A., Sutskever, I., and Salakhutdinov, R. Dropout: A simple way to prevent neural networks from overfitting. *Journal of Machine Learning Research*, 15(56):1929–1958, 2014. URL <http://jmlr.org/papers/v15/srivastava14a.html>.

Svetunkov, I. *Complex exponential smoothing*. Lancaster University (United Kingdom), 2016.

Tay, Y., Bahri, D., Metzler, D., Juan, D.-C., Zhao, Z., and Zheng, C. Synthesizer: Rethinking self-attention for transformer models. In *International Conference on Machine Learning*, pp. 10183–10192. PMLR, 2021.

Taylor, S. J. and Letham, B. Forecasting at scale. *The American Statistician*, 72(1):37–45, 2018.

Theodosiou, M. Forecasting monthly and quarterly time series using stl decomposition. *International Journal of Forecasting*, 27(4):1178–1195, 2011.

Tsai, Y.-H. H., Bai, S., Yamada, M., Morency, L.-P., and Salakhutdinov, R. Transformer dissection: An unified understanding for transformer’s attention via the lens of kernel. In *Proceedings of the 2019 Conference on Empirical Methods in Natural Language Processing and the 9th International Joint Conference on Natural Language Processing (EMNLP-IJCNLP)*, pp. 4344–4353, Hong Kong, China, November 2019. Association for Computational Linguistics. doi: 10.18653/v1/D19-1443. URL <https://aclanthology.org/D19-1443>.

Vaswani, A., Shazeer, N., Parmar, N., Uszkoreit, J., Jones, L., Gomez, A. N., Kaiser, Ł., and Polosukhin, I. Attention is all you need. In *Advances in neural information processing systems*, pp. 5998–6008, 2017.

Vlachos, M., Yu, P., and Castelli, V. On periodicity detection and structural periodic similarity. In *Proceedings of the 2005 SIAM international conference on data mining*, pp. 449–460. SIAM, 2005.

Winters, P. R. Forecasting sales by exponentially weighted moving averages. *Management science*, 6(3):324–342, 1960.

Wu, H., Xu, J., Wang, J., and Long, M. Autoformer: Decomposition transformers with Auto-Correlation for long-term series forecasting. In *Advances in Neural Information Processing Systems*, 2021.

Wu, S., Xiao, X., Ding, Q., Zhao, P., Wei, Y., and Huang, J. Adversarial sparse transformer for time series forecasting. In *NeurIPS*, 2020.

You, W., Sun, S., and Iyyer, M. Hard-coded gaussian attention for neural machine translation. *arXiv preprint arXiv:2005.00742*, 2020.

Zerveas, G., Jayaraman, S., Patel, D., Bhamidipaty, A., and Eickhoff, C. A transformer-based framework for multivariate time series representation learning. In *Proceedings of the 27th ACM SIGKDD Conference on Knowledge Discovery & Data Mining*, pp. 2114–2124, 2021.

Zhou, H., Zhang, S., Peng, J., Zhang, S., Li, J., Xiong, H., and Zhang, W. Informer: Beyond efficient transformer for long sequence time-series forecasting. In *Proceedings of AAAI*, 2021.

A. Exponential Smoothing Attention

A.1. Further Details on ESA Implementation

Algorithm 2 PyTorch-style pseudocode of naive \mathcal{A}_{ES}

```

mm: matrix multiplication, outer: outer product
repeat: einops style tensor operations, gather: gathers values along an
axis specified by dim

# V: value matrix, shape: L x d
# v0: initial state, shape: d
# alpha: smoothing parameter, shape: 1

L, d = V.shape

# obtain exponentially decaying weights
powers = arange(L) # L
weight = alpha * (1 - alpha).pow(flip(powers)) # L

# perform a strided roll operation
# rolls a matrix along the columns in a strided manner
# i.e. first row is shifted right by L-1 positions,
# second row is shifted L-2, ..., last row is shifted by 0.
weight = repeat(weight, 'L -> T L', T=L) # L x L
indices = repeat(arange(L), 'L -> T L', T=L)
indices = (indices - (arange(L) + 1).unsqueeze(1)) % L
weight = gather(weight, dim=-1, index=indices)

# triangle masking to achieve the exponential smoothing
# attention matrix
weight = triangle_causal_mask(weight)

output = mm(weight, V)

init_weight = (1 - alpha) ** (powers + 1)
init_output = outer(init_weight, v0)

return init_output + output

```

Algorithm 3 PyTorch-style pseudocode of conv1d_fft

```

next_fast_len: find the next fast size of input data to fft, for zero-
padding, etc.
rfft: compute the one-dimensional discrete Fourier Transform for real
input
x.conj(): return the complex conjugate, element-wise
irfft: computes the inverse of rfft
roll: roll array elements along a given axis
index_select: returns a new tensor which index es the input tensor
along dimension dim using the entries in index

# V: value matrix, shape: L x d
# weight: exponential smoothing attention vector, shape: L
# dim: dimension to perform convolution on

# obtain lengths of sequence to perform convolution on
N = V.size(dim)
M = weight.size(dim)

# Fourier transform on inputs
fast_len = next_fastlen(N + M - 1)
F_V = rfft(V, fast_len, dim=dim)
F_weight = rfft(weight, fast_len, dim=dim)

# multiplication and inverse
F_V.weight = F_V * F_weight.conj()
out = irfft(F_V.weight, fast_len, dim=dim)
out = out.roll(-1, dim=dim)

# select the correct indices
idx = range(fast_len - N, fast_len)
out = out.index_select(dim, idx)

return out

```

Algorithm 2 describes the naive implementation for ESA by first constructing the exponential smoothing attention matrix, \mathcal{A}_{ES} , and performing the full matrix-vector multiplication. Efficient \mathcal{A}_{ES} relies on Algorithm 3, to achieve an $\mathcal{O}(L \log L)$ complexity, by speeding up the matrix-vector multiplication. Due to the structure lower triangular structure of \mathcal{A}_{ES} (ignoring the first column), we note that performing a matrix-vector multiplication with it is equivalent to performing a convolution with the last row. Algorithm 3 describes the pseudocode for fast convolutions using fast Fourier transforms.

A.2. Level Smoothing via Exponential Smoothing Attention

$$\begin{aligned}
\mathbf{E}_t^{(n)} &= \alpha * (\mathbf{E}_t^{(n-1)} - \mathbf{S}_t^{(n)}) + (1 - \alpha) * (\mathbf{E}_{t-1}^{(n)} + \mathbf{B}_{t-1}^{(n)}) \\
&= \alpha * (\mathbf{E}_t^{(n-1)} - \mathbf{S}_t^{(n)}) + (1 - \alpha) * \mathbf{B}_{t-1}^{(n)} + (1 - \alpha) * [\alpha * (\mathbf{E}_{t-1}^{(n-1)} - \mathbf{S}_{t-1}^{(n)}) + (1 - \alpha) * (\mathbf{E}_{t-2}^{(n)} + \mathbf{B}_{t-2}^{(n)})] \\
&= \alpha * (\mathbf{E}_t^{(n-1)} - \mathbf{S}_t^{(n)}) + \alpha * (1 - \alpha) * (\mathbf{E}_{t-1}^{(n-1)} - \mathbf{S}_{t-1}^{(n)}) + (1 - \alpha) * \mathbf{B}_{t-1}^{(n)} + (1 - \alpha)^2 * \mathbf{B}_{t-2}^{(n)} \\
&\quad + (1 - \alpha)^2 [\alpha * (\mathbf{E}_{t-2}^{(n-1)} - \mathbf{S}_{t-2}^{(n)}) + (1 - \alpha) * (\mathbf{E}_{t-3}^{(n)} + \mathbf{B}_{t-3}^{(n)})] \\
&\quad \vdots \\
&= (1 - \alpha)^t (\mathbf{E}_0^{(n)} - \mathbf{S}_0^{(n)}) + \sum_{j=0}^{t-1} \alpha * (1 - \alpha)^j * (\mathbf{E}_{t-j}^{(n-1)} - \mathbf{S}_{t-j}^{(n)}) + \sum_{k=1}^t (1 - \alpha)^k * \mathbf{B}_{t-k}^{(n)} \\
&= \mathcal{A}_{\text{ES}}(\mathbf{E}_{t-L:t}^{(n-1)} - \mathbf{S}_{t-L:t}^{(n)}) + \sum_{k=1}^t (1 - \alpha)^k * \mathbf{B}_{t-k}^{(n)}
\end{aligned}$$

Based on the above expansion of the level equation, we observe that $\mathbf{E}_n^{(t)}$ can be computed by a sum of two terms, the first of which is given by an \mathcal{A}_{ES} term, and we finally, we note that the second term can also be calculated using the conv1d_fft algorithm, resulting in a fast implementation of level smoothing.

B. Discrete Fourier Transform

The DFT of a sequence with regular intervals, $\mathbf{x} = (x_0, x_1, \dots, x_{N-1})$ is a sequence of complex numbers,

$$c_k = \sum_{n=0}^{N-1} x_n \cdot \exp(-i2\pi kn/N),$$

for $k = 0, 1, \dots, N-1$, where c_k are known as the Fourier coefficients of their respective Fourier frequencies. Due to the conjugate symmetry of DFT for real-valued signals, we simply consider the first $\lfloor N/2 \rfloor + 1$ Fourier coefficients and thus we denote the DFT as $\mathcal{F} : \mathbb{R}^N \rightarrow \mathbb{C}^{\lfloor N/2 \rfloor + 1}$. The DFT maps a signal to the frequency domain, where each Fourier coefficient can be uniquely represented by the amplitude, $|c_k|$, and the phase, $\phi(c_k)$,

$$|c_k| = \sqrt{\Re\{c_k\}^2 + \Im\{c_k\}^2} \quad \phi(c_k) = \tan^{-1} \left(\frac{\Im\{c_k\}}{\Re\{c_k\}} \right)$$

where $\Re\{c_k\}$ and $\Im\{c_k\}$ are the real and imaginary components of c_k respectively. Finally, the inverse DFT maps the frequency domain representation back to the time domain,

$$x_n = \mathcal{F}^{-1}(\mathbf{c})_n = \frac{1}{N} \sum_{k=0}^{N-1} c_k \cdot \exp(i2\pi kn/N),$$

C. Implementation Details

C.1. Hyperparameters

For all experiments, we use two layers of encoders and their two corresponding decoder stacks. The model dimension is set to 512, while the feedforward layer dimension is set to 2048. The number of heads in multi-head exponential smoothing attention is set to 8. The kernel size for input embedding is 3. We perform hyperparameter tuning by performing a grid search over learning rate, lookback window size, and number of frequencies K . For learning rate, we use the tuning range $\{1e-3, 3e-4, 1e-4, 3e-5, 1e-5\}$, and for K , a tuning range of $\{0, 1, 2, 3\}$. The tuning range for lookback window size depends on the datasets. For ETTh datasets, $\{96, 168, 336, 720\}$, for ETTm, $\{96, 192, 288, 672\}$, for Traffic, Weather, ECL, and Exchange, $\{168, 336, 720\}$, and for ILI, $\{24, 36, 48, 60\}$.

C.2. Optimization

We use the Adam optimizer (Kingma & Ba, 2015) with $\beta_1 = 0.9$, $\beta_2 = 0.999$, and $\epsilon = 1e-08$, and a batch size of 32. We schedule the learning rate with linear warmup over 3 epochs, and cosine annealing thereafter for a total of 15 training epochs for all datasets. The minimum learning rate is set to $1e-30$. For smoothing and damping parameters, we set the learning rate to be 100 times larger and do not use learning rate scheduling.

C.3. Regularization

We apply two forms of regularization during the training phase.

Data Augmentations We utilize a composition of three data augmentations, applied in the following order - scale, shift, and jitter, activating with a probability of 0.5.

1. Scale – The time-series is scaled by a single random scalar value, obtained by sampling $\epsilon \sim \mathcal{N}(0, 0.2)$, and each time step is $\tilde{x}_t = \epsilon x_t$.
2. Shift – The time-series is shifted by a single random scalar value, obtained by sampling $\epsilon \sim \mathcal{N}(0, 0.2)$ and each time step is $\tilde{x}_t = x_t + \epsilon$.
3. Jitter – I.I.D. Gaussian noise is added to each time step, from a distribution $\epsilon_t \sim \mathcal{N}(0, 0.2)$, where each time step is now $\tilde{x}_t = x_t + \epsilon_t$.

Dropout We apply dropout (Srivastava et al., 2014) with a rate of $p = 0.2$ across the model. Dropout is applied on the outputs of the Input Embedding, Frequency Self-Attention and Multi-Head ES Attention blocks, in the Feedforward block (after activation and before normalization), on the attention weights, as well as damping weights.

D. Datasets

ETT² Electricity Transformer Temperature (ETT) (Zhou et al., 2021) is a multivariate time-series dataset, comprising of load and oil temperature data recorded every 15 minutes from electricity transformers. ETT consists of two variants, ETTm and ETTh, whereby ETTh is the hourly-aggregated version of ETTm, the original 15 minute level dataset.

ECL³ Electricity Consuming Load (ECL) measures the electricity consumption of 321 households clients over two years, the original dataset was collected at the 15 minute level, but is pre-processed into an hourly level dataset.

Exchange⁴ Exchange (Lai et al., 2018) tracks the daily exchange rates of eight countries (Australia, United Kingdom, Canada, Switzerland, China, Japan, New Zealand, and Singapore) from 1990 to 2016.

Traffic⁵ Traffic is an hourly dataset from the California Department of Transportation describing road occupancy rates in San Francisco Bay area freeways.

Weather⁶ Weather measures 21 meteorological indicators like air temperature, humidity, etc., every 10 minutes for the year of 2020.

ILI⁷ Influenza-like Illness (ILI) records the ratio of patients seen with ILI and the total number of patients on a weekly basis, obtained by the Centers for Disease Control and Prevention of the United States between 2002 and 2021.

E. Synthetic Dataset

The synthetic dataset is constructed by a combination of trend and seasonal component. Each instance in the dataset has a lookack window length of 192 and forecast horizon length of 48. The trend pattern follows a nonlinear, saturating pattern, $b(t) = \frac{1}{1+\exp \beta_0(t-\beta_1)}$, where $\beta_0 = -0.2$, $\beta_1 = 192$. The seasonal pattern follows a complex periodic pattern formed by a sum of sinusoids. Concretely, $s(t) = A_1 \cos(2\pi f_1 t) + A_2 \cos(2\pi f_2 t)$, where $f_1 = 1/10$, $f_2 = 1/13$ are the frequencies, $A_1 = A_2 = 0.15$ are the amplitudes. During training phase, we use an additional noise component by adding i.i.d. gaussian noise with 0.05 standard deviation. Finally, the i -th instance of the dataset is $x_i = [x_i(1), x_i(2), \dots, x_i(192 + 48)]$, where $x_i(t) = b(t) + s(t + i) + \epsilon$.

²<https://github.com/zhouhaoyi/ETDataset>

³<https://archive.ics.uci.edu/ml/datasets/ElectricityLoadDiagrams20112014>

⁴<https://github.com/laiguokun/multivariate-time-series-data>

⁵<https://pems.dot.ca.gov/>

⁶<https://www.bgc-jena.mpg.de/wetter/>

⁷<https://gis.cdc.gov/grasp/fluview/fluportaldashboard.html>

F. Multivariate Forecasting Benchmark

Table 4. Multivariate forecasting results on all datasets. Best results are highlighted in bold.

METHODS	ETSFOMER	AUTOFORMER	INFORMER	LOGTRANS	REFORMER	LSTNET	LSTM								
METRICS	MSE	MAE	MSE	MAE	MSE	MAE	MSE	MAE	MSE	MAE	MSE	MAE			
ETTH1	24	0.374 0.411	0.384	0.425	0.577	0.549	0.686	0.604	0.991	0.754	1.293	0.901	0.650	0.624	
	48	0.378 0.414	0.392	0.419	0.685	0.625	0.766	0.757	1.313	0.906	1.456	0.960	0.702	0.675	
	168	0.443 0.450	0.490	0.481	0.931	0.752	1.002	0.846	1.824	1.138	1.997	1.214	1.212	0.867	
	336	0.755	0.671	0.505 0.484	1.128	0.873	1.362	0.952	2.117	1.280	2.655	1.369	1.424	0.994	
	720	0.761	0.663	0.498 0.500	1.215	0.896	1.397	1.291	2.415	1.520	2.143	1.380	1.960	1.322	
ETTH2	24	0.190 0.296	0.261	0.341	0.720	0.665	0.828	0.750	1.531	1.613	2.742	1.457	1.143	0.813	
	48	0.245 0.326	0.312	0.373	1.457	1.001	1.806	1.034	1.871	1.735	3.567	1.687	1.671	1.221	
	168	0.387 0.410	0.457	0.455	3.489	1.515	4.070	1.681	4.660	1.846	3.242	2.513	4.117	1.674	
	336	0.429 0.452	0.471	0.475	2.723	1.340	3.875	1.763	4.028	1.688	2.544	2.591	3.434	1.549	
	720	0.453 0.472	0.474	0.484	3.467	1.473	3.913	1.552	5.381	2.015	4.625	3.709	3.963	1.788	
ETTM1	24	0.262 0.337	0.383	0.403	0.323	0.369	0.419	0.412	0.724	0.607	1.968	1.170	0.621	0.629	
	48	0.336 0.379	0.454	0.453	0.494	0.503	0.507	0.583	1.098	0.777	1.999	1.215	1.392	0.939	
	96	0.368 0.392	0.481	0.463	0.678	0.614	0.768	0.792	1.433	0.945	2.762	1.542	1.339	0.913	
	288	0.408 0.420	0.634	0.528	1.056	0.786	1.462	1.320	1.820	1.094	1.257	2.076	1.740	1.124	
	672	0.471 0.452	0.606	0.542	1.192	0.926	1.669	1.461	2.187	1.232	1.917	2.941	2.736	1.555	
ETTM2	24	0.110 0.222	0.153	0.261	0.173	0.301	0.211	0.332	0.333	0.429	1.101	0.831	0.580	0.572	
	48	0.142 0.250	0.178	0.280	0.303	0.409	0.427	0.487	0.558	0.571	2.619	1.393	0.747	0.630	
	96	0.183 0.275	0.255	0.339	0.365	0.453	0.768	0.642	0.658	0.619	3.142	1.365	2.041	1.073	
	288	0.291 0.339	0.342	0.378	1.047	0.804	1.090	0.806	2.441	1.190	2.856	1.329	0.969	0.742	
	672	0.395 0.402	0.434	0.430	3.126	1.302	2.397	1.214	3.090	1.328	3.409	1.420	2.541	1.239	
ECL	96	0.187 0.302	0.201	0.317	0.274	0.368	0.258	0.357	0.312	0.402	0.680	0.645	0.375	0.437	
	192	0.196 0.311	0.222	0.334	0.296	0.386	0.266	0.368	0.348	0.433	0.725	0.676	0.442	0.473	
	336	0.215 0.330	0.231	0.338	0.300	0.394	0.280	0.380	0.350	0.433	0.828	0.727	0.439	0.473	
	720	0.236 0.348	0.254	0.361	0.373	0.439	0.283	0.376	0.340	0.420	0.957	0.811	0.980	0.814	
EXCHANGE	96	0.083 0.202	0.197	0.323	0.847	0.752	0.968	0.812	1.065	0.829	1.551	1.058	1.453	1.049	
	192	0.180 0.302	0.300	0.369	1.204	0.895	1.040	0.851	1.188	0.906	1.477	1.028	1.846	1.179	
	336	0.354 0.433	0.509	0.524	1.672	1.036	1.659	1.081	1.357	0.976	1.507	1.031	2.136	1.231	
	720	0.996 0.761	1.447	0.941	2.478	1.310	1.941	1.127	1.510	1.016	2.285	1.243	2.984	1.427	
TRAFFIC	96	0.614	0.395	0.613	0.388	0.719	0.391	0.684	0.384	0.732	0.423	1.107	0.685	0.843	0.453
	192	0.629	0.398	0.616	0.382	0.696	0.379	0.685	0.390	0.733	0.420	1.157	0.706	0.847	0.453
	336	0.646	0.417	0.622	0.337	0.777	0.420	0.733	0.408	0.742	0.420	1.216	0.730	0.853	0.455
	720	0.631 0.389	0.660	0.408	0.864	0.472	0.717	0.396	0.755	0.423	1.481	0.805	1.500	0.805	
WEATHER	96	0.189 0.272	0.266	0.336	0.300	0.384	0.458	0.490	0.689	0.596	0.594	0.587	0.369	0.406	
	192	0.231 0.303	0.307	0.367	0.598	0.544	0.658	0.589	0.752	0.638	0.560	0.565	0.416	0.435	
	336	0.305 0.357	0.359	0.395	0.578	0.523	0.797	0.652	0.639	0.596	0.597	0.587	0.455	0.454	
	720	0.352 0.391	0.419	0.428	1.059	0.741	0.869	0.675	1.130	0.792	0.618	0.599	0.535	0.520	
ILI	24	2.862 1.128	3.483	1.287	5.764	1.677	4.480	1.444	4.400	1.382	6.026	1.770	5.914	1.734	
	36	2.683 1.029	3.103	1.148	4.755	1.467	4.799	1.467	4.783	1.448	5.340	1.668	6.631	1.845	
	48	2.456 0.986	2.669	1.085	4.763	1.469	4.800	1.468	4.832	1.465	6.080	1.787	6.736	1.857	
	60	2.630 1.057	2.770	1.125	5.264	1.564	5.278	1.560	4.882	1.483	5.548	1.720	6.870	1.879	

G. Univariate Forecasting Benchmark

Table 5. Univariate forecasting results on all datasets. Best results are highlighted in bold.

METHODS	ETSFOMER	AUTOFORMER	INFORMER	N-BEATS	DEEPAR	ARIMA	PROPHET					
METRICS	MSE	MAE	MSE	MAE	MSE	MAE	MSE	MAE	MSE	MAE	MSE	MAE
ETTH1	24	0.036 0.144	0.052	0.181	0.098	0.247	0.094	0.238	0.107	0.28	0.108	0.284
	48	0.056 0.181	0.081	0.224	0.158	0.319	0.210	0.367	0.162	0.327	0.175	0.424
	168	0.076 0.218	0.118	0.273	0.183	0.346	0.232	0.391	0.239	0.422	0.396	0.504
	336	0.077 0.226	0.138	0.292	0.222	0.387	0.232	0.388	0.445	0.552	0.468	0.593
	720	0.112 0.265	0.135	0.291	0.269	0.435	0.322	0.490	0.658	0.707	0.659	0.766
ETTH2	24	0.089 0.234	0.106	0.255	0.093	0.24	0.198	0.345	0.098	0.263	3.554	0.445
	48	0.119 0.272	0.135	0.287	0.155	0.314	0.234	0.386	0.163	0.341	3.19	0.474
	168	0.199	0.360	0.186 0.341	0.232	0.389	0.331	0.453	0.255	0.414	2.8	0.595
	336	0.218 0.384	0.244	0.388	0.263	0.417	0.431	0.508	0.604	0.607	2.753	0.738
	720	0.216 0.378	0.299	0.440	0.277	0.431	0.437	0.517	0.429	0.58	2.878	1.044
ETTM1	24	0.020	0.115	0.020 0.110	0.030	0.137	0.054	0.184	0.091	0.243	0.09	0.206
	48	0.025 0.121	0.033	0.141	0.069	0.203	0.190	0.361	0.219	0.362	0.179	0.306
	96	0.030 0.130	0.052	0.177	0.194	0.372	0.183	0.353	0.364	0.496	0.272	0.399
	288	0.067 0.197	0.091	0.240	0.401	0.554	0.186	0.362	0.948	0.795	0.462	0.558
	672	0.093 0.228	0.104	0.259	0.512	0.644	0.197	0.368	2.437	1.352	0.639	0.697
ECL	48	0.304	0.410	0.375	0.452	0.239	0.359	0.551	0.392	0.204 0.357	0.879	0.764
	168	0.332	0.423	0.477	0.526	0.447	0.503	0.893	0.538	0.315	0.436	1.032
	336	0.393 0.461	0.658	0.610	0.489	0.528	1.035	0.669	0.414	0.519	1.136	0.876
	720	0.533 0.565	0.898	0.710	0.540	0.571	1.548	0.881	0.563	0.595	1.251	0.933
EXCHANGE	96	0.126 0.268	0.241	0.387	0.591	0.615	0.156	0.299	0.417	0.515	0.112 0.245	0.828
	192	0.206 0.341	0.273	0.403	1.183	0.912	0.669	0.665	0.813	0.735	0.304	0.404
	336	0.436 0.503	0.508	0.539	1.367	0.984	0.611	0.605	1.331	0.962	0.736	0.598
	720	1.320	0.887	0.991 0.768	1.872	1.072	1.111	0.860	1.894	1.181	1.871	0.935